CHEMICAL COMPOSITION, TENSILE PROPERTIES AND STRUCTURAL CHARACTERIZATION OF BURITI FIBER

HEITOR LUIZ ORNAGHI JÚNIOR,[*,**,***] ÁLVARO GUSTAVO DE OLIVEIRA MORAES,[*] MATHEUS POLETTO,[*,**] ADEMIR JOSÉ ZATTERA[**] and SANDRO CAMPOS AMICO[*]

[*]*PPGE3M, Federal University of Rio Grande do Sul, 9500, Bento Gonçalves Av., 91501-970, Porto Alegre, Rio Grande do Sul, Brazil*
[**]*PGEPROTEC, Caxias do Sul University, 95070-560, Caxias do Sul, Rio Grande do Sul, Brazil*
[***]*PGMAT, Engineering and Materials Science Graduate Program, Caxias do Sul University, 95070-490, Caxias do Sul, Rio Grande do Sul, Brazil*
✉ *Corresponding author: Heitor Luiz Ornaghi Júnior, ornaghijr.heitor@yahoo.com*

Received June 17, 2014

In recent years, increasing attention has been given to the use of plant fibers in composite materials due to environmental concerns. These studies may lead to its wide-spread use as reinforcement in composite materials. In this work, chemical composition, moisture content, Fourier transform infrared spectroscopy (FTIR), X-ray diffraction (XRD), thermogravimetry, mechanical testing and morphological studies were performed for the characterization of buriti fiber. Chemical analysis revealed a high amount of lignin and extractives. FTIR analysis demonstrated that buriti fiber contains high moisture content and thermal stability reached around 200 °C. XRD showed that buriti exhibits mainly cellulose I structure with a crystallinity index of 44.6% and 51.9% (depending on the method used). Its tensile properties are similar to those of other plant fibers and morphological studies indicated surface defects in the longitudinal section associated with a porous structure.

Keywords: buriti fibers, chemical composition, crystallinity, thermal analysis, morphology

INTRODUCTION

It is well known that plant fibers are attractive reinforcements for different types of polymer matrix composites.[1-3] There are some advantages in using these vegetable fibers for this application, including low specific weight, higher specific strength and stiffness, environmentally friendly character, low density, non-toxicity, greater efficiency in sound absorption and fracture resistance when compared to glass fibers.[4-6] However, there are drawbacks, such as high moisture absorption and poor mechanical properties, which limit their use.[7,8,9-12]

Additional motivation for the use of plant fibers in composites is related to increasing environmental concerns by governments, such as those of the European Union, imposing recent laws on the use of about 95% of recyclable materials – with about 85% renewable materials – in all new automotive parts to achieve the "end of life" required by 2015.[13] These composites may sometimes reach comparable performance with composites reinforced with inorganic synthetic glass fibers.[14] Besides, when lignocellulosic fibers are used in composites, developing countries which usually produce them, further integrate in the global composite industry as developers and manufacturers, with increased revenues and employment.[13,15] A large amount of data on the structure and properties of a variety of lignocellulosic fibers (including some Brazilian fibers) is available in the literature, some of them are compiled in Table 1. Depending on the fiber composition, there are differences in their physical and chemical properties, which can ultimately result in composites with different characteristics. The search for new and suitable plant fibers for composites has led to the study of Buriti (*Mauritia flexuosa L.f.*), which belongs to the *Arecaceae* family and the *Mauritia* genus, and is widely available in the North and Northeast

regions of Brazil.[16] This dioecious tropical palm has high ecological, cultural and economic value, mainly due to the valuable oil extracted from its fruit, which is used by the cosmetic industry.[16,17]

In addition, the fibers extracted from the tree leaf could be used as reinforcement in composites. Buriti palm tree and fiber are shown in Fig. 1, as well the characteristic extraction and processing stages.[18]

Just a few studies can be found in the literature addressing the characteristics of the buriti fiber.[19,20] So, this study focused on the physical-chemical and structural characterization of the buriti fiber aiming to promote its use as reinforcement for composite materials.

EXPERIMENTAL

The leaf buriti fiber used in this study was obtained as yarns from Sisalsul Fibras Naturais (Caxias do Sul/RS, Brazil). The sample was dried in a vacuum oven for 24 h at 105 °C prior to testing. The samples were ground to a fine powder of 200 μm in a Wiley-mill prior to TGA, XRD and FTIR analyses.

The amount of extractives in the buriti fiber was determined via Soxhlet extraction in triplicate using ethanol/benzene (from Vetec Chemical) and ethanol and hot water, during 4 h for each solvent, according to Tappi T204 cm-97 standard. The Klason lignin content was determined according to Tappi T222 cm-02 standard using sulphuric acid (from Vetec Chemical). The ash content was determined in a muffle furnace at 600 °C for 1 h, based on Tappi T211om-02 standard. The holocellulose content (cellulose + hemicellulose) was determined by difference using the extractives, lignin and ash content.

The moisture content of the fibers was determined according to ASTM D2654-89, using an oven at 105 ± 1 °C for 2 h. The thermogravimetric analysis (TGA50 – Shimadzu) was carried out under N_2 atmosphere with a purge gas flow of 50 $cm^3.min^{-1}$ from 25 to 800 °C. Approximately 10 mg of sample was used and the heating rate used was 10 °C.min^{-1}, following ASTM E1131-08.

FTIR spectra were obtained using a Nicolet IS10 – Thermo Scientific spectrometer. Fiber powder (c.a. 5 mg) was dispersed in a KBr matrix (100 mg) and pressed to produce pellets. Data collection followed 32 scans in the range of 4000 to 400 cm^{-1} at a resolution of 4 cm^{-1}. The fiber was oven-dried in vacuum at 105 °C for 24 h prior to producing pellets.

X-ray diffractograms were collected using a sample holder mounted on a Shimadzu diffractometer (XRD-6000), with monochromatic Cu*K*α radiation (λ = 0.1542 nm), operating at 40 kV and 30 mA. Intensities were measured in the range of 5° < 2θ < 35°, typically with scan steps of 0.05° and 2 $s.step^{-1}$ (1.5° min^{-1}). The crystallinity index was determined either by calculating the area of the three major peaks and dividing them by the entire curve area, as proposed by Hermans and described in the study reported by Poletto,[21] or following the Segal method,[22] which is based on the height of the highest diffraction peak, and the height of the minimum intensity between the major peaks.[23] The *d*-spacing was calculated by Gaussian deconvolution and the crystallite size was calculated using the Scherrer equation. [23]

Conditioning of the fibers for the mechanical testing was carried out according to ASTM D1776-08. Tensile tests (BS ISO 11566:1996) were carried out in a dynamic mechanical analyzer (DMA, TA Instruments, model 2980) in the controlled force mode using a tension film clamp to hold the single-filament specimen. The ramp force and the gauge length were kept constant, namely 5 N/min and 15 mm, respectively, and a pre-load of 0.1 N was used. The constant Δ(force)/time test program was used and all tests were conducted at 26 °C with 1 min isothermal prior to each test. Nine useful fibers were tested, their cross-section was assumed circular for simplification and their diameter was measured with a Mitutoyo dial thickness gage (0.01 mm resolution) and used in the calculations.

The surface cross-section of oven dried (at 70 °C with air circulation for 24 h) fibers was examined using a Scanning Electron Microscope (Shimadzu Superscan SS-550). The fibers were mounted on aluminum holders using double-sided electrically conductive carbon adhesive tabs and the fibers were sputtered with a layer of gold prior to analysis.

RESULTS AND DISCUSSION

Chemical composition

The chemical composition of the buriti fiber is presented in Table 2. The holocellulose content is in agreement with that of other plant fibers (see Table 1). The amount of lignin is within the upper limit in comparison with most fibers (with lignin content around 10 wt%), which may indicate higher stiffness[24] for the buriti fiber since lignin is a randomized condensed polymer with many aromatic rings with very high molecular weight.[25,21]

On the other hand, buriti fiber presented higher content of extractives, which are compounds of low molecular mass that can degrade at relatively low temperatures[25,26] and even during processing, leading to undesirable composite properties, such as browning and decreased mechanical strength.[26] The ash content was higher than usually reported in the literature.

Table 1
Chemical composition, mechanical and physical properties of plant fibers

Fiber	Cellulose (wt%)	Hemicellulose (wt%)	Lignin (wt%)	Extractives (wt%)	Ash (wt%)	References
Kenaf	31-72	20.3-23	9-19	2.5	--	[17,18, 24, 25]
Jute	45-71	13.6-21	12-26	2.5	0.7-1.0	[16-19, 20, 24, 25]
Sisal	65-67	12	9.9	1-4	0.1-0.9	[18, 19, 22, 25]
Ramie	68.6-91	5-16.7	0.6-0.7	6-6.5	--	[16-19, 20, 22, 25]
Curaua	71-74	9.9-21	7.5-11	3.5-3.8	0.8-0.9	[20, 22, 25]
Fiber	Moisture content (%)	Elastic modulus (GPa)	Tensile strength (MPa)	Specific strength ($MPa.g^{-1}.cm^{3}$)	Strain at break (%)	References
Kenaf	--	53	930	--	1.6	[17, 25]
Jute	12.5-13.7	10-30	393-800	280-610	1.5-1.8	[17-19, 23-25]
Sisal	1.2	9.0-38	400-700	320-530	2.0-14	[17-19, 21, 25]
Ramie	7.5-17	24.5-128	220-938	270-620	2.0-3.8	[17-19, 21, 25]
Curaua	9.1	11.8	500-1150	360-820	3.7-4.3	[17, 21, 25, 27]

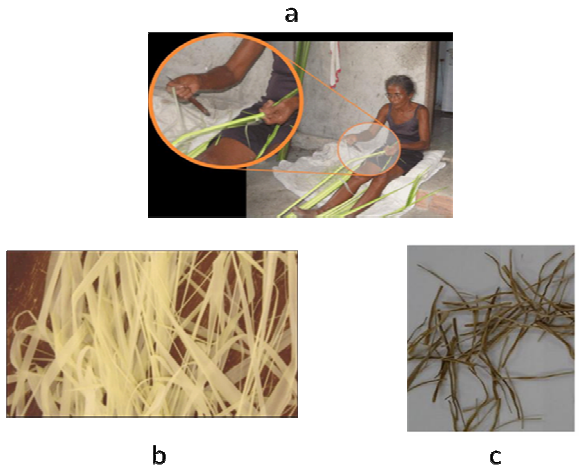

Figure 1: Production of buriti fiber yarn: a) buriti fiber extraction, b) newly extracted *in natura* buriti fiber and c) buriti fiber as received by the supplier

These differences are understandable considering that the chemical composition of lignocellulosic fibers depends on various factors, such as species, variety, type of soil, weather conditions, part of the plant from which the fibers are extracted, plant age among others.[13,27]

Moisture content

The obtained moisture content of the buriti fiber (Table 2) is in agreement with that of other natural fibers (see Table 1). The fiber moisture content is important for composite processing because moisture influences adhesion between fibers and the polymeric matrix.[28] Hemicelluloses are mainly responsible for moisture absorption in plant fibers, but cellulose and lignin also contribute.[29] Moisture sorption leads to swelling of the cell wall and consequently fiber swelling until saturation is reached.[30] Beyond this point, free water accumulates in the void spaces of the fiber. So, high moisture content may be associated with a highly porous fiber structure.

Thermal analysis

Fig. 2 shows the results of the thermo-gravimetry analysis of the buriti fiber. The DTG curve reveals four distinct degradation peaks, where the first (around 50-100 °C) is related to the release of water retained in the fiber. This weight loss corresponds to around 9%, which is in agreement with the measured moisture content.

A more prominent degradation process starts at around 200 °C, three peaks being noticed at 280 °C, 333 °C and 406 °C, which are usually assigned to the decomposition of hemicellulose, cellulose and lignin, respectively.[30] According to Kim *et al.*,[31] the depolymerization of hemicellulose occurs in the range of 180-350 °C, the random cleavage of the glycosidic linkage of cellulose between 275-350 °C and the degradation of lignin between 200-500 °C. It is important to mention that the lignin peak is more prominent than that of the majority of the fibers found in literature and this is in agreement with the high lignin content of the buriti fiber.

IR spectroscopy

The FTIR spectrum of buriti fiber is shown in Fig. 3. To allow better visualization, the spectrum was split into two main regions, namely: the OH and CH stretching vibrations in the 4000-2500 cm^{-1} region (Fig. 3a) and the fingerprint region, which is assigned to the stretching vibrations of different groups from buriti components in the 2000-800 cm^{-1} region (Fig. 3b).

Figure 3a shows a strong O-H stretching band at 3430 cm^{-1} associated with free or hydrogen-bonded hydroxyl groups in cellulose[32,33] along with asymmetric and symmetric CH_2 stretching at 2920 and 2850 cm^{-1},[13,21,34] respectively. Figure 3b shows a typical band at 1740 cm^{-1} assigned to the C=O stretching of carboxylic groups of hemicellulose.[13,34]

Table 2
Chemical composition (%) and moisture content (%) of buriti fiber

Fiber	Holocellulose	Lignin	Extractives	Ash	Moisture content
Buriti	67.8 ± 3.0	24.0 ± 3.0	5.7 ± 0.3	2.5 ± 0.1	9.1± 0.3

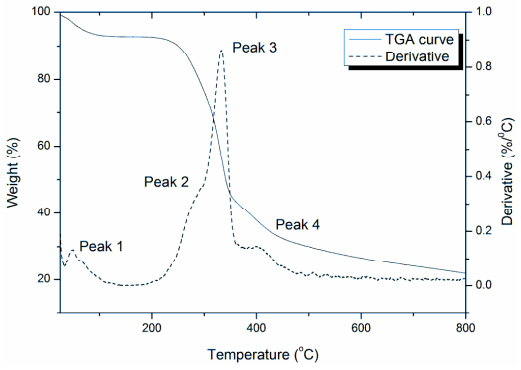

Figure 2: TGA and DTG curves of buriti fiber

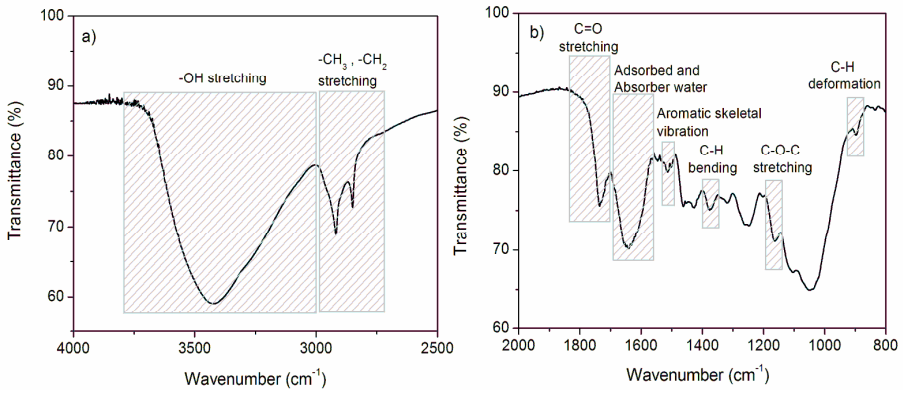

Figure 3: FTIR spectrum in (a) 4000-2500 cm^{-1} and (b) 2000-800 cm^{-1} regions

A prominent band is seen at 1642 cm^{-1}, assigned to C=O aldehyde stretching vibration and also to adsorbed and absorbed water,[35] which may corroborate the higher amount of water in the fiber, as discussed before. The band at 1510 cm^{-1} is related to the aromatic skeletal vibration of lignin, while the peaks at 1424, 1374, 1317, 1240, 1161, 1040 and 897 cm^{-1} are assigned to C-H, C-O and C-O-C deformation, bending, or stretching vibrations of many groups in lignin and carbohydrates.[13,21] A comparison between the buriti fiber and the buriti oil spectra can be found in Albuquerque's study.[34]

X-ray diffractometry

Figure 4 shows the X-ray diffractogram of the buriti fiber. The crystallographic planes are labeled according to the native cellulose structure, as described by Wada and Okano.[36] Three distinct diffraction peaks can be noted, the first two being at $2\theta \approx 14.8°$ and 16.1°, assigned to the $(1\bar{1}0)$ and (110) crystallographic planes.[31] Considering that the contribution of the peak at $2\theta \approx 34.3°$ assigned to the (004) crystallographic plane is very small in comparison with the other peaks,[37] it was not taken into account in the calculations. The peak at $2\theta \approx 21.9°$ assigned to the (200) crystallographic plane and the d-spacing associated with the three main peaks (5.99, 5.51 and 4.06 Å, respectively) indicate that buriti fiber is mainly composed of cellulose I, a typical plant structure.[26,36,38]

The degree of cellulose crystallinity is one of the most important structure parameters in plant fibers.[26] The rigidity of cellulosic fibers increases and their flexibility decreases with the increase in the ratio of crystalline to amorphous regions.[26,39] The calculated crystallinity index as proposed by Hermans and described in a study performed by Poletto[21] was approximately 44.6% and, using the Segal method,[40] approximately 51.90%, which is in the lower range of values usually found in the literature for plant fibers (47-75%). The relatively low crystallinity index indicates that buriti fiber has less ordered cellulose regions than sisal and ramie fibers, for instance, which can be justified by its higher lignin content. The crystallite size of the (002) crystalline plane was calculated according to the Scherrer equation and a value of 2.84 nm was found, which indicates a small crystallite size and corroborates with the low crystallinity index of the buriti fiber.

Tensile properties

For the tensile testing, only fibers within the 150-170 μm range of diameter were used, avoiding major deviations and reducing scatter in tensile strength. This is close to the mean diameter reported by Santos *et al.*[11] for the buriti fiber, 182 ± 6 μm.

Figure 5 shows a typical stress-strain curve obtained for the buriti fiber during DMA testing and the linear region between the middle and the end of this curve was used to calculate the elastic modulus, usually around 1.0-1.7% strain.

The curvature seen in this curve may indicate the viscoelastic nature of the fiber[40] and to understand this behavior it is necessary to consider that plant fibers, such as buriti, are regarded as natural composites. In this case, the crystalline cellulose microfibrils, considered reinforcements, are helically wound in an amorphous lignin matrix and these lignocellulosic fibers show an overall viscoelastic behavior under loading.

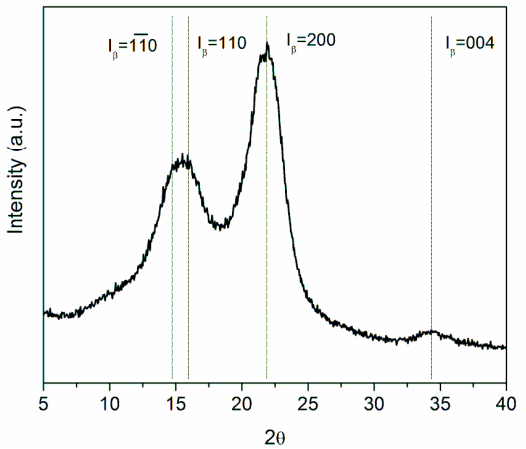

Figure 4: XRD of buriti fiber

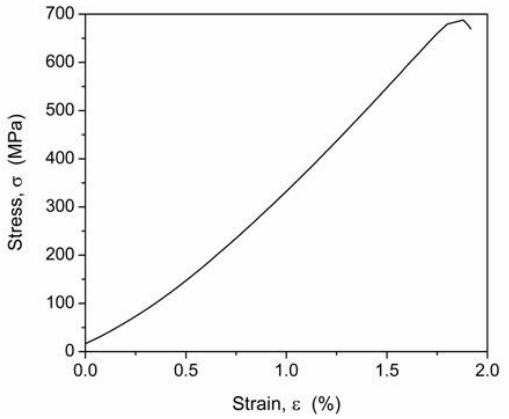

Figure 5: Typical stress-strain curve obtained for buriti fiber

Table 3
Tensile properties of buriti fiber

Fiber	Ultimate load (N)	Tensile strength (MPa)	Elastic modulus (GPa)	Strain at break (%)
Buriti	14.77 (± 3.38)	735 (± 168)	27 (± 5)	2.7 (± 0.4)

Accordingly, the applied stress is shared between crystalline and non-crystalline constituents of the fiber. The spiral-like structure of the fiber undergoes deformation, with initial uncoiling of microfibrils followed by matrix yielding and slippage of molecules with increasing applied stress, leading to decohesion of crystalline and non-crystalline molecules mainly on their weak-links or imperfections.[40] In addition, the extent to which such a fiber resists deformation in the low strain region also depends on fiber age and origin.

The results for ultimate load, tensile strength, elastic modulus and strain at break of the buriti fiber are presented in Table 3. These values are similar to those found for other natural fibers (see Table 1).

Indeed, there are several reports in the literature on the tensile behavior of sisal and curaua fibers.[4,24,27,28,35] For sisal fiber, the diameter, tensile strength, elastic modulus and elongation at break usually vary within 125-250 μm, 233-589 MPa, 9.3-27.3 GPa and 2.8-4.9%, respectively,[4] which are somewhat similar to the properties of curaua fiber.[35] These references mention that strength and modulus decrease with increasing fiber diameter and fiber length.[35] Thus, the difference found between the tensile strength values of this study (735 MPa) compared to the previous work[11] (271 MPa) can be partly explained by the difference in fiber length (15 mm and 50 mm, respectively).

It is expected that more crystalline lignocellulosic fibers present higher tensile strength and modulus.[36,39] Buriti fiber has low crystallinity (at about 45%) compared with other natural fibers such as sisal and curaua (around 70%), even so it showed similar tensile properties, which is perhaps related to the higher amount of lignin in buriti.[40] The extra lignin may protect the fiber and avoid cellulose degradation during fiber extraction from the plant.

Morphological aspect

SEM micrographs of the buriti fiber surface are shown in Fig. 6. In Fig. 6a, the micrograph of the longitudinal section reveals that buriti has a smooth surface with some defects associated with a porous structure, as shown in detail in Fig. 6b.

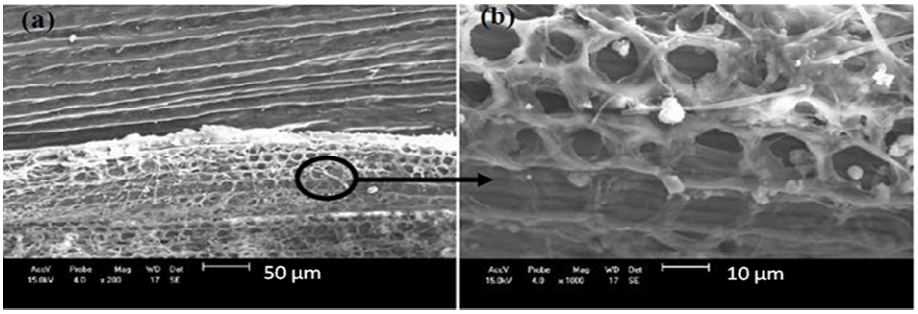

Figure 6: SEM micrographs of buriti fiber in longitudinal section at ×200 (a) and detail of the porous structure at ×1000 (b)

This porous structure helps justifying the high water absorption, which is undesirable when this fiber is used in composites. It can be also noted that the fibers are composed of individual elementary fibers, like ramie, jute or other bast fibers, and not of single cells, as in the case of cotton.

CONCLUSION

Chemical analysis revealed that buriti fiber contains a higher amount of lignin and extractives than other natural fibers. FT-IR indicated that buriti fiber also contains a higher amount of adsorbed and absorbed water, which is in agreement with the higher weight loss observed by TGA around 100 °C. Thermal analysis results showed that a more prominent fiber degradation process occurs at around 200 °C and XRD patterns revealed that buriti fiber is mainly composed of cellulose I structure with crystallinity index of 44.6-51.9%. The fiber mechanical properties are similar to those of other natural fibers and morphological studies showed a smooth longitudinal surface with some surface defects associated with a porous structure.

ACKNOWLEDGEMENTS: The authors would like to thank CNPq, CAPES, and FAPERGS for the financial support.

REFERENCES

[1] H. L. Ornaghi Jr., A. S. Bolner, R. Fiorio, A. J. Zattera, and S. C. Amico, *J. Appl. Polym. Sci*., **118**, 887 (2010).
[2] C. Borsoi, L. C. Scienza, and A. J. Zattera, *J. Appl. Polym. Sci*., **128**, 653 (2013).
[3] D. Romanzini, H. L. Ornaghi Jr., S. C. Amico, A. J. Zattera, *J. Reinf. Plast. Comp*., **31**, 1652 (2012).
[4] A. G. O. Moraes, M.-R. Sierakowski, T. M. Abreu, and S. C. Amico, *Compos. Interfaces*, **18**, 407 (2011).
[5] H. L. Ornaghi Jr., H. S. P. da Silva, A. J. Zattera, S. C.Amico, *J. Appl. Polym. Sci*., **125**, E110 (2012).
[6] A. R. Sena Neto, M. A. M. Araujo, F. V. D. Souza, L. H. C. Mattoso, and J. M. Marconcini, *Ind. Crop. Prod*., **43**, 529 (2013).
[7] N. Cordeiro, C. Gouveia, and J. M. Jacob, *Ind. Crop. Prod*., **33**, 108 (2011).
[8] M. Poletto, M. Zeni, and A. J. Zattera, *J. Thermoplast. Comp*., **25**, 821 (2011).
[9] J. H. S Almeida Jr., H. L. Ornaghi Jr., S. C. Amico, and F. D. R. Amado, *Mater. Design*, **42**, 111 (2012).
[10] V. Pistor, S. S. S. Soares, H. L. Ornaghi Jr., R. Fiorio, and A. J. Zattera, *Mat. Res*., **15**, 1 (2012).
[11] R. S. Santos, A. A. de Souza, M.-A. de Paoli, and C. M. L. de Souza, *Compos.: A-Appl. S*., **41**, 1123 (2010).
[12] A. G. O. Moraes, M.-R. Sierakowski, and S. C. Amico, *Fiber Polym*., **13**, 641 (2012).
[13] J. L. Guimarães, E. Frollini, C. G. da Silva, F. Wypych, and K. G. Satyanarayana, *Ind. Crop. Prod*., **30**, 407 (2009).
[14] D. Romanzini, A. Lavoratti, H. L.Ornaghi Jr., S. C. Amico, and A. J. Zattera, *Mater. Design*, **47**, 9 (2013).
[15] A. S. Fonseca, F. A. Mori, G. H. D. Tonoli, H. Savastano Jr., D. L. Ferrari *et al*., *Ind. Crop. Prod*., **47**, 43 (2013).
[16] L. F. França, G. Reber, M. A. A. Meireles, N. T. Machado, and G. Brunner, *J. Supercrit. Fluid.*, **14**, 247 (1999).
[17] H. H. F. Koolen, F. M. A. da Silva, F. C. Gozzo, A. Q. L. de Souza, and A. D. L.de Souza, *Food. Res. Int*., **51**, 467 (2013).
[18] S. N. Monteiro, V. Calado, F. M. Margem, and R. J. S. Rodriguez, *J. Mater. Res. Tech*., **1**, 189 (2012).
[19] S. N. Monteiro, V. Calado, R. J. S. Rodriguez, and F. M. Margem, *J. Mater. Res. Tech*., **1**, 117 (2012).
[20]www.artesanatocomdesign.blogspot.com.br., accessed on 07/22/2014.
[21] M. Poletto, A. J. Zattera, M. M. C. Forte, and R. M. C. Santana, *Bioresour. Technol*., **109**, 148 (2012).
[22] A. D. French, *Cellulose*, **21**, 885 (2013).
[23] A. D. French, M. Santiago Cintrón, *Cellulose*, **20**, 583 (2013).

[24] M. J. John and S. Thomas, *Carbohyd. Polym*., **71**, 343 (2008).
[25] A. N. Shebani, A. N. van Reenen, and M. Meincken *Thermochim. Acta*, **471**, 43 (2008).
[26] M. Poletto, A. J. Zattera, R. M. C. Santana, *J. Appl. Polym. Sci*., **126**, E336 (2012).
[27] K. G. Satyanarayana, J. L. Guimarães, and F. Wypych, *Compos.*: *A-Appl. S*., **38**, 1694 (2007).
[28] M. A. S. Spinacé, C. S. Lambert, K. K. G. Fermoselli, M.-A. De Paoli, *Carbohyd. Polym*., **77**, 47 (2009).
[29] E. M. F. Aquino, L. P. S. Sarmento, W. Oliveira, and R. V. Silva, *J. Reinf. Plast. Comp*., **26**, 219 (2007).
[30] H. Teng and Y. C. Wei, *Ind. Eng. Chem. Res*., **37**, 3806 (1998).
[31] H.-S. Kim, S. Kim, H.-J. Kim, and H.-S. Yang, *Thermochim. Acta*, **451**, 181 (2006).
[32] T. Kondo, *Cellulose*, **4**, 281 (1997).
[33] D. Dai, and M. Fan, *Vib. Spectrosc*., **55**, 300 (2011).
[34] M.L.S. Albuquerque, I. Guedes, P. Alcantara Jr., S.G.C. Moreira, *Vib. Spectrosc*., **33**, 127 (2003).
[35] F. Tomczak, K. G. Satyanarayana and T. H. D. Sydenstricker, *Compos.*: *A-Appl. S*., **38**, 2227 (2007).
[36] M. Wada and T. Okano, *Cellulose*, **8**, 183 (2001).
[37] H. L. Ornaghi Jr., A. J. Zattera, and S. C. Amico, *Cellulose*, **21**, 189 (2014).
[38] H. L. Ornaghi Jr., M. Poletto, A. J. Zattera, and S. C. Amico, *Cellulose*, **21**, 177 (2014).
[39] E. Gümüskaya, M. Usta, and H. Kirei, *Polym. Degrad. Stabil*., **81**, 559 (2003).
[40] F. Tomczak, T. H. D. Sydenstricker, and K. G. Satyanarayana, *Compos.*: *A-Appl. S*., **38**, 1710 (2007).